

RSC Advances



This is an *Accepted Manuscript*, which has been through the Royal Society of Chemistry peer review process and has been accepted for publication.

Accepted Manuscripts are published online shortly after acceptance, before technical editing, formatting and proof reading. Using this free service, authors can make their results available to the community, in citable form, before we publish the edited article. This *Accepted Manuscript* will be replaced by the edited, formatted and paginated article as soon as this is available.

You can find more information about *Accepted Manuscripts* in the [Information for Authors](#).

Please note that technical editing may introduce minor changes to the text and/or graphics, which may alter content. The journal's standard [Terms & Conditions](#) and the [Ethical guidelines](#) still apply. In no event shall the Royal Society of Chemistry be held responsible for any errors or omissions in this *Accepted Manuscript* or any consequences arising from the use of any information it contains.



Journal Name

ARTICLE

Structural Characterization, Optical Properties and Photocatalytic Activity of MOF-5 and its Hydrolysis Products: Implications on their Excitation Mechanism.

Received 00th January 20xx,
Accepted 00th January 20xx

DOI: 10.1039/x0xx00000x

www.rsc.org/

N. A. Rodríguez,^a R. Parra^{a,b} and M. A. Grela^a

The existing concerns on the limited stability of Zn₄O-based MOFs upon exposure to humidity or aqueous environments, as well as on the excitation mechanisms, are discussed on the basis of Raman, FTIR, DR-UV and XRD measurements. This paper demonstrates that MOF-5 dispersed in water produces a relatively stable new phase, MOF-5W, which slowly degrades to MOF-5H, a mixture of MOF-5W and zinc terephthalate dihydrate (ZTDH). The structure and optical properties of MOF-5W and MOF-5H and their optical and photocatalytic properties reveal the main role played by the organic moiety in determining the final properties of these structures, supporting the idea of a ligand to ligand charge transfer (LLCT) excitation mechanism rather than the usually assumed ligand to metal charge transfer (LMCT).

Introduction

Metal-Organic Frameworks (MOFs) are hybrid materials constituted by metal-based clusters coordinated to organic ligands¹. MOFs are excellent materials for a variety of applications such as gas storage², drug-delivery³, and catalysis⁴. The interest in these materials is based on their high porosity and surface area, as well as the possibility of tuning its optical and electronic properties by changing the inorganic and/or the organic moieties⁵. Particularly, the photocatalytic behaviour characteristics of metal-organic frameworks have recently received considerable attention, from both fundamental aspects and practical applications^{6,7}. Some of these studies involve MOF-5, a well-known MOF made up by Zn₄O clusters linked by the conjugated base of terephthalic acid [H₂BDC = benzenedicarboxylic acid]⁸ (See Figure 1).

Despite the fact that MOF-5 is a widely studied material, there are still unsolved issues about its optical properties, its semiconductor characteristics and, specially, its photocatalytic performance. The first reports on this regard⁹⁻¹² indicated that MOF-5 would have semiconductor-like properties, with a

bandgap of 3.4 eV ($\lambda_{\text{BG}} = 365 \text{ nm}$) and a green photoluminescence, with a maximum at 525 nm. These results were accounted by invoking a ligand to cluster -or ligand to metal- charge transfer (LCCT/LMCT) in which Zn₄O units behave as ZnO quantum dots⁹⁻¹². However, it has been recognized that the synthetic strategy employed to obtain MOF-5 in the first studies¹³ produces extrinsic ZnO nanoparticles and/or zinc species within the pores of the lattice^{14,15}. Thus, the semiconductor properties of MOF-5, and its excitation mechanism have been severely questioned¹⁵. Recently, a photoelectrochemical study¹⁶ using MOF-5 films free from ZnO demonstrated the existence of photoinduced currents whose action spectra nearly matches the diffuse reflectance absorption of the films. However, the absorption onset of MOF-5 appears at shorter wavelengths (310 nm). This 55 nm blue shift in comparison with first reports is consistent with a ligand to ligand charge-transfer rather than a metal to ligand excitation mechanism, as commonly accepted^{5,17}. Thus, these issues certainly need revision.

Another point of controversy originates from the use of MOF-5 as a photocatalyst in aqueous media¹⁰, considering its liability to hydrolysis. In fact, it has been reported that the exposure of MOF-5 to water¹¹ or moisture^{11,13,18-19} leads to distinctive products with well defined XRD patterns and reduced porosity,^{13,20,21} which will be named in the following as MOF-5W and MOF-5H, respectively. The stability of MOF-5 under such conditions is a topic of renewed interest^{20,21}.

^a Departamento de Química, Facultad de Ciencias Exactas y Naturales, Universidad Nacional de Mar del Plata, Mar del Plata, Argentina.

^b Instituto de Investigaciones en Ciencia y Tecnología de Materiales (INTEMA), CONICET-UNMDP, Mar del Plata, Argentina.

† magrela@mdp.edu.ar

Electronic Supplementary Information (ESI) available: XRD patterns of dry MOF-5, MOF-5H in DMF, MOF-69C and ZTDH. See DOI: 10.1039/x0xx00000x

Within this context, the aims of this work are to assess the optical properties, stability and photoinduced redox behaviour of MOF-5, MOF-5W and MOF-5H and to evaluate the potential use of these materials as photocatalysts. For these purposes, measurements and experiments were performed under careful control of the experimental conditions to ensure the integrity of the prepared materials. To analyse the photocatalytic activity of the metal organic frameworks, the oxidation of a molecular probe, (2,2,6,6-tetramethylpiperidin-1-yl)oxyl (TEMPO), was followed in air saturated suspensions by EPR spectroscopy. The premise behind the selection of TEMPO as a model compound lies in the fact that it provides a simple analytical method to determine very low conversions with high accuracy and selectivity.

The paper is organized as follows: First, XRD and Raman analyses of MOF-5 exposed to water and controlled levels of humidity (MOF-5W or MOF-5H depending on the exposure time) are presented in order to elucidate the changes in the structure and composition of the original metal-organic framework. Then, the optical properties of these materials and the organic precursor are analysed to determine the pertinence of the LMCT excitation mechanism. Finally, the photochemical oxidation of TEMPO by irradiation of MOF-5/MOF-5W/MOF-5H is analysed to scrutinize the role of the ligand in their photocatalytic activity.

Experimental Section

Materials.

Terephthalic acid (Sigma), zinc acetate dihydrate (Fluka), TEMPO (Aldrich) and triethylamine (Sintorgan) were of the highest purity available and used as received. Chloroform and N,N-dimethylformamide (DMF, chromatographic grade) were purchased from Sintorgan and used without further purification.

Sample preparation.

MOF-5 was synthesized following a previously described procedure²². Briefly, terephthalic acid (0.304g; 1.83 mmol) and triethylamine (0.5 ml) were dissolved in DMF (25 ml). Additionally, zinc acetate dihydrate (1.019 g; 4.64 mmol) was dissolved in another recipient with DMF (30 ml). The latter solution was added to the former during 15 minutes under vigorous stirring. The mixture was further stirred for another 2 h, after which the precipitate was separated by centrifugation (9000 rpm, 15 min), washed three times and dispersed in DMF. To obtain MOF-5W, MOF-5 dispersion was centrifuged and washed twice with water. Finally, the solid was resuspended in water (10 ml) and stored.

The MOF-5H sample was prepared by centrifuging a MOF-5 slurry and washing it twice with chloroform. The solid was allowed to dry and then transferred to a closed recipient containing a beaker with a mixture of ethylene glycol - water (50:50) to set the humidity around 70-80% (measured by a hygrometer).

Characterization.

Samples were characterized by the techniques described below. Except when indicated, MOF-5 (MOF-5W) samples were kept damp in DMF (water) during the analysis.

XRD patterns were recorded from a PANalytical X'Pert diffractometer under $K\alpha$ copper radiation. Calculated XRD pattern for MOF-5 was obtained from crystal data using the PowderCell 2.3 software suite^{8,23}.

Raman spectroscopy was carried out with a Renishaw inVia spectrometer equipped with a near-IR (785 nm) excitation diode laser. MOF-5 sample for Raman analysis was prepared by washing the dispersion with chloroform twice and then mixing the damp solid with dry KCl in a mortar. The sample was stored in a desiccator until analysed. Fourier Transformed Infrared Spectroscopy (FTIR) was carried out by means of a Nicolet 6700 spectrometer (Thermo Electron Corporation) in Attenuated Total Reflectance (ATR) mode.

Samples for diffuse UV-VIS and photoluminescence spectra were placed between two silica-glass slides. Diffuse UV-Vis spectra were recorded on a Shimadzu UV-2450 spectrometer equipped with an integrating sphere accessory. Photoluminescence spectra were obtained on a PTI QM4 Fluorescence System operating with a xenon lamp. The incident beam was placed at 30° from the normal of the slides containing the samples.

EPR spectra for quantitative analysis of TEMPO were obtained at ambient temperature using a Bruker ELEXSYS E500T spectrometer operating at X-band (Data acquisition parameters: N° of points: 1024; Central Field: 348 mT; Field sweep: 3 mT; Number of scans: 5; Microwave power: 20.5 mW; Modulation frequency: 100 kHz; Sweep time: 90 s; Modulation amplitude: 2 Gpp).

Photocatalytic studies.

Room-temperature, air saturated slurries of the different photocatalysts dispersed in DMF or H₂O, as appropriate, (photocatalyst concentration: 4.8 g/L) contained in square silica-glass cells (Volume = 3cm³) were fully illuminated with monochromatic radiation. For this purpose, the output of a 1000 W Hg/Xe high-pressure lamp, was dispersed by a high-intensity grating monochromator (Schoeffel-Kratos) using a 10 nm bandwidth. A magnetic stirring bar was used to assure proper mixing and aeration during irradiation. Well determined volumes (20 μ l and 10 μ l for the organic and aqueous slurries, respectively) of the suspension were withdrawn from the cell and transferred to thin cylindrical silica tubes in order to record the EPR spectrum of the sample. The amount of TEMPO was calculated from the intensity of the double integrated central EPR-signal at $g = 2.0071$ ²⁴.

Results and Discussion

Characterization of the samples.

Figure 2 shows the XRD pattern of the as prepared materials along with a reference pattern of MOF-5 calculated using reported crystal data^{2,8,22}. The experimental and calculated

patterns of MOF-5 show perfect agreement. In order to track the possible presence of impurities and/or alterations in MOF-5, the first two diffraction peaks (at $2\theta = 6.9^\circ$ and 9.7°) are commonly analysed. Hafizovic *et al.*¹⁴ showed that an inversion of the relative intensities at these angles is produced because of the occurrence of zinc species within the pores of the metal-organic framework. However, changes in the relative intensities of the peaks are also observed when drying pure MOF-5 under vacuum, and preserving it from humidity^{16-18,25,26} (See Figure S1). Thus, MOF-5 samples were kept damp in DMF during the XRD analysis as reported elsewhere²². MOF-5 remains stable (for months) when stored in anhydrous DMF, *i.e.*, its XRD pattern is not altered.

As mentioned above, dispersion of MOF-5 in water produces a new phase^{13,18,26}. The transformation of MOF-5 into MOF-5W can be monitored by the disappearance of the XRD peaks at $2\theta = 6.9^\circ$ and 9.7° and the appearance of a new one at $2\theta = 8.8^\circ$ (see Figure 2c). Greathouse *et al.*²⁷ proposed that water induces peripheral Zn-O bond breakdown and framework distortion.

However, the crystalline structure of MOF-5W is still unsolved, probably because of the difficulty in obtaining single-crystals. Although it has been suggested that MOF-5 gives place to MOF-69C (which presents a different cluster morphology)²⁸⁻³⁰ when exposed to humidity, the comparison between their respective XRD patterns reveals clear differences (Figure S2). On this regard, it is remarkable that MOF-5 can be partially recovered from MOF-5W or MOF-5H if resuspended in DMF at room temperature (Figure S3). This fact supports the idea that MOF-5 and MOF-5H have similar structures and that the main difference between both phases is the partial linkage of peripheral Zn-O bonds (see Scheme 1).

MOF-5W can be stored in an aqueous dispersion for at most 10 days, without apparent changes in its XRD pattern. However, it slowly decomposes into MOF-5H (Scheme 1). MOF-5H is also obtained when MOF-5 is exposed to humid air (70-80%) for at least 96 hours, as pointed out in the *experimental section*. The XRD pattern of this new solid clearly shows the presence of MOF-5W plus new peaks marked with asterisks, see Figure 2. A close inspection to the work of Thirumurugan *et al.*³¹ shows that the second phase is zinc terephthalate dihydrate, ZTDH. Besides, ZTDH was synthesized and the matching of the peaks was confirmed (Figure S4). This simple analysis reveals that the final product of MOF-5 hydrolysis, MOF-5H, is actually a mixture of two phases, MOF-5W and ZTDH (Scheme 1), contrary to the belief that MOF-5H is a single phase of formula $\text{ZnBDC}\cdot x\text{H}_2\text{O}$ ³².

Raman spectra of MOF-5, MOF-5W and MOF-5H are shown in Figure 3. The similarity between MOF-5 and MOF-5W structures is in accordance with the nearly identical spectra of both materials. Particularly, the Raman analysis of both MOF-5 and MOF-5W show a signal at 1435 cm^{-1} which is ascribed to the existence of peripheral Zn-O bonds³³, suggesting that the proposed linkage between Zn-O is not complete, as mentioned before. This result contrasts with the disappearance of this band in the FTIR spectra as shown in S5. This observation is in agreement with previous data³³ and perhaps reflects a change

in the transition probability produced by the distortion of the structure. That is to say, peripheral Zn-O linkage cannot be easily observed by vibrational measurements, because there are still many of them in MOF-5W, as pointed out in Scheme 1. This assumption is supported by further evidence as discussed in the following section.

Finally, it is worth to remark that Raman spectra of MOF-5, MOF-5W and MOF-5H do not show the phonon modes ascribed to crystalline or amorphous ZnO ¹⁶. This result, together with the absence of a green luminescence in the emission spectra of MOF-5, MOF-5W and MOF-5H (Figure 4), allows confirming that the samples are free from ZnO ¹⁵.

Optical Properties.

Absorption spectra were obtained from the diffuse reflectance spectra as $A=1-R-T$, where R stands for the reflected and T for the transmitted light ratio. As observed in Figure 5, the absorption spectrum of MOF-5 shows a sharp increment near 320 nm.

The optical band gap may be assessed by different procedures³⁴. As a first approximation, the band gap energy (E_g) can be estimated directly by extrapolating the long-wavelength edge of the peak in the absorbance spectrum to zero. More properly, it can be obtained by analyzing the dependence of the absorbance with the photon energy, according to the nature of the semiconductor (direct or indirect)³⁵. The result obtained for MOF-5 (usually considered as a direct semiconductor) indicates that $E_g(\text{MOF-5}) = 3.86\text{ eV}$ (Figure 6). This result, although in agreement with recent reports,^{5,16} is about 0.5 eV higher than the first measurements of MOF-5 band gap ($\sim 3.4\text{ eV}$)⁹⁻¹² which are still employed as reference for theoretical analysis and calculations of the optical properties of this material^{36,37}. However, even though calculations predict E_g values for MOF-5 near 3.4 eV, they favour the idea that the excitation is mainly localized in the ligand^{36,38}.

On the other hand, the single argument in favour of a LMCT mechanism is based in the red-shift observed in the spectra of the organic linker (obtained for a 2 mM solution of H_2BDC in dimethyl sulfoxide)⁵ in comparison with MOF-5. However, the analysis presented in Figure 6 indicates that solid H_2BDC has a lower optical band gap (3.58 eV) than that observed in the homogeneous solution (4 eV)⁵. Thus, considering the absorption of the solids, a blue-shift is actually observed.

Diffuse reflectance spectrum of MOF-5W shows a red-shift respect to MOF-5 and a more gradual increment near the band edge of the absorption spectrum (Figure 5). The slow increment in the absorption suggests that MOF-5W would be an indirect semiconductor³⁵. Tauc plot of MOF-5W leads to $E_g(\text{MOF-5W}) = 3.37\text{ eV}$. No significant differences were found in MOF-5H absorption spectrum (data not shown) with respect to MOF-5W.

ZTDH absorption spectrum was also recorded (Figure S6). The optical bandgap was assessed to be 3.41 eV. The differences in the band-gap between MOF-5 and MOF-5H, or MOF-5W may be accounted by invoking a partial protonation of the ligand, in

line with the differences observed for H₂BDC with respect to BDC²⁻ solutions (Figure S7).

However, dissimilar π - π stacking in solids may also contribute to the observed differences in the absorption spectra caused by the lower distance between the organic moieties. This argument is necessary to account for the behaviour observed for ZTDH.

Photocatalytic properties.

The photocatalytic activity of the samples was investigated by studying the degradation of TEMPO in air saturated slurries of MOF-5 in DMF, and MOF-5H and MOF-5W in water. TEMPO is a stable free radical with a triplet signature ascribed to the nitrogen hyperfine coupling constant, $a_N = 17.1$ G. The EPR spectrum of TEMPO dissolved in pure DMF and water shows nearly identical g-factors ($g = 2.0071$). Besides, no changes in the EPR spectra could be detected by dissolving the nitroxide in slurries of the different photocatalysts. Blank experiments confirmed that TEMPO did not decompose in absence of light and/or metal-organic frameworks within the elapsed time of these experiments.

The proposed mechanism for TEMPO photooxidation is shown in Scheme 2. TEMPO is oxidized by photogenerated holes, while oxygen removes the electrons from the conduction band³⁹.

Figure 7 shows the differences between TEMPO decomposition rates in presence of MOF-5, under irradiation at various wavelengths. It is evident that irradiation at 330 nm cannot induce charge separation and neither did irradiation at 350 nm. On the other hand, the different MOF-5 photocatalytic activity, changing the excitation wavelength to 320 and 303 nm, can be accounted by the higher absorption of this material at these wavelengths. The above result supports the higher value of E_g derived in this work, and contradicts previous reports^{9,10}.

An estimation of the photonic efficiency for TEMPO degradation (ζ) relative to commercial ZnO (see Figure 7) indicates a value of $\zeta(\text{MOF-5}) / \zeta(\text{ZnO}) [\%] = 26\%$, at the same irradiation wavelength (320 nm) and the same mass of photocatalyst. Quantitative results on the photocatalytic behaviour of MOFs are seldom found in the literature, and often involve aqueous dispersions of the photocatalyst^{10,11}. For example, Alvaro *et al.*¹⁰ determined that the rate of phenol degradation using an aqueous dispersion of MOF-5 is nearly three times lower than that observed by irradiation of ZnO. However, MOF-5W or MOF-5H may have been present during the photocatalytic characterization carried out in Alvaro's work due to the assessed limited stability of MOF-5 in water. Thus, the degradation of TEMPO using MOF-5W and MOF-5H materials dispersed in water was analysed in this work.

Surprisingly, we observed that under the same conditions (4.8 g/L of the photocatalyst, $\lambda_{\text{irr}}=320$ nm) the photocatalytic degradation of TEMPO in MOF-5H was about 4 times faster than using MOF-5W or ZTDH alone. Thus, the higher efficiency of MOF-5H may be ascribed to a synergistic effect between the

two phases whose contact promotes charge separation. It should be noted that both phases, MOF-5W and ZTDH, have the ligand excitation as the main contribution to their photocatalytic activity. These conclusions are derived considering the partial linkage between Zn-O bonds in MOF-5H which would decrease the effect of LMCT (if it ever occurs). Additionally, a LMCT mechanism in ZTDH is unlikely due to the high charge localization required in a single atom.

Conclusions

The fate of MOF-5 in humid and aqueous environments was scrutinized by detailed XRD, Raman and UV-VIS spectra analysis. It was determined that the final structure of MOF-5 in water (MOF-5H) consists in a mixture of a distorted and partially hydrolysed MOF-5 (MOF-5W) and ZTDH. Furthermore, the optical and photocatalytic experimental evidences (blue-shift observed in the absorption spectrum on going from H₂BDC to MOF-5 and the higher efficiency observed for TEMPO in MOF-5H compared with MOF-5W) could not be accounted by invoking a LMCT excitation mechanism, but rather highlights the main role played by ligands in determining the final properties of those compounds supporting a LLCT mechanism. MOF-5 behaves as a semiconductor, preserving its structure in anhydrous organic solvents. Also, MOF-5H, is capable of photoinduce redox processes in aqueous media. Apparently, the presence of two phases in this material favours charge separation.

Acknowledgements

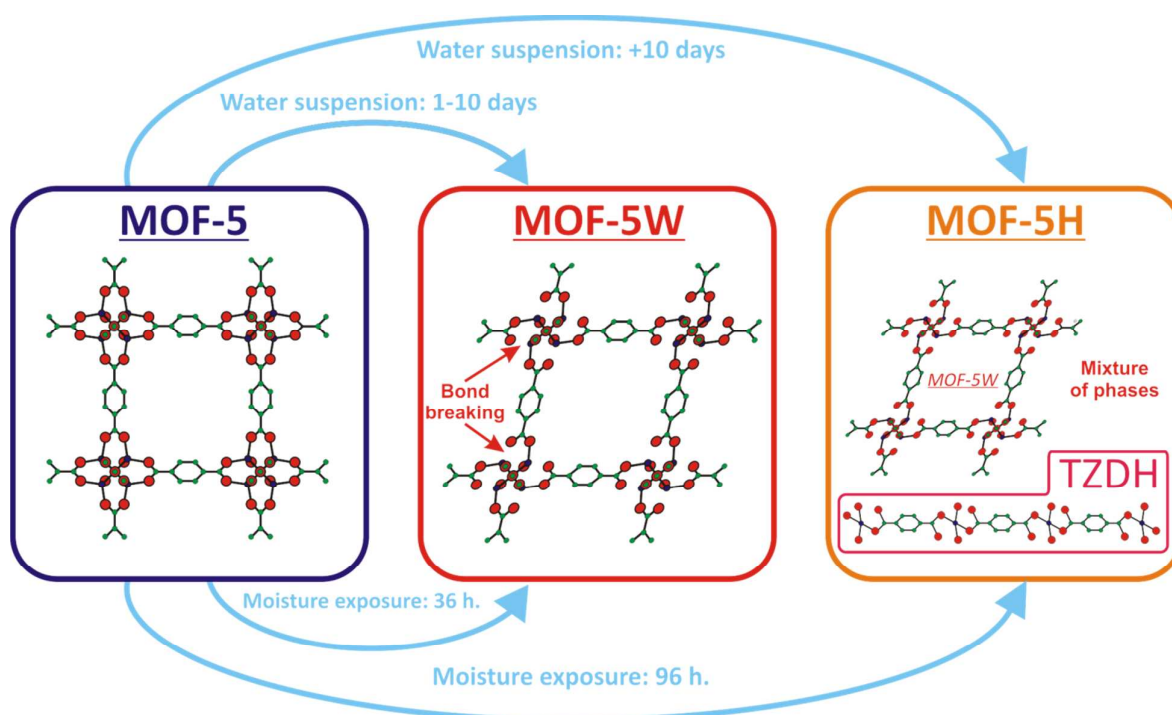
The authors thank P. Botta (INTEMA, CONICET) for technical assistance in XRD analysis. This work was financially supported by CONICET (project PIP 467), and ANPCyT (PICT 1456/13). R. P. and M. A. G. are members of the research staff of CONICET, Argentina. N.A.R thanks CONICET for a doctoral fellowship.

Notes and references

- 1 N. Stock, S. Biswas, *Chem. Rev.*, 2012, **112**, 933-969.
- 2 M. Eddaoudi, J. Kim, N. Rosi, D. Vodak, J. Wachter, M. O'Keeffe, O. M. Yaghi, *Science*, 2002, **295**, 469-472.
- 3 P. Horcajada, R. Gref, T. Baati, P. K. Allan, G. Maurin, P. Couvreur, G. R. Ferey, R. E. Morris, C. Serre, *Chem. Rev.* 2011, **112**, 1232-1269.
- 4 J. Gascon, A. Corma, F. Kapteijn, F. X. Llabrés i Xamena, *ACS Catal.*, 2014, **4**, 361-378.
- 5 C. K. Lin, D. Zhao, W. Y. Gao, Z. Yang, J. Ye, T. Xu, Q. Ge, S. Ma, D. J. Liu, *Inorg. Chem.*, 2012, **51**, 9039-9044.
- 6 C. Wang, Z. Xie, K. E. deKrafft, W. Lin, *J. Am. Chem. Soc.*, 2011, **133**, 13445-13454.
- 7 T. Zhang, W. Lin, *Chem. Soc. Rev.* 2014, **43**, 5982-5993.
- 8 H. Li, M. Eddaoudi, M. O'Keeffe, O. M. Yaghi, *Nature*, 1999, **402**, 276-279.
- 9 S. Bordiga, C. Lamberti, G. Ricchiardi, L. Regli, F. Bonino, A. Damin, K. P. Lillerud, M. Bjorgen, A. Zecchina, *Chem. Commun.*, 2004, **40**, 2300-20301.
- 10 M. Alvaro, E. Carbonell, B. Ferrer, F. X. Llabrés i Xamena, H. Garcia, *Chem. Eur. J.*, 2007, **13**, 5106-5112.

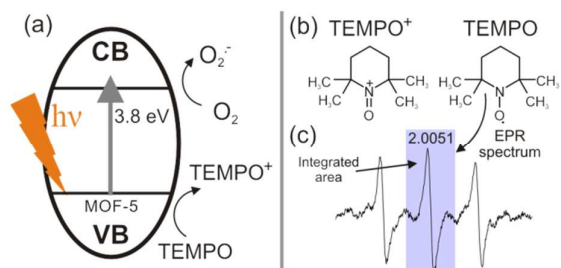
- 11 T. Tachikawa, J. R. Choi, M. Fujitsuka, T. Majima, *J. Phys. Chem. C*, 2008, **112**, 14090-14101.
- 12 F. X. Llabrés i Xamena, A. Corma, H. García, *J. Phys. Chem. C*, 2007, **111**, 80-95.
- 13 L. Huang, H. Wang, J. Chen, Z. Wang, J. Sun, D. Zhao, Y. Yan, *Micropor. Mesopor. Mat.*, 2003, **58**, 105-114.
- 14 J. Hafizovic, M. Bjorgen, U. Olsbye, P. D. C. Dietzel, S. Bordiga, C. Prestipino, C. Lamberti, K. P. Lillerud, *J. Am. Chem. Soc.*, 2007, **129**, 3612-3620.
- 15 P. L. Feng, J. J. Perry Iv, S. Nikodemski, B. W. Jacobs, S. T. Meek, M. D. Allendorf, *J. Am. Chem. Soc.*, 2010, **132**, 15487-15489.
- 16 J. I. Feldblyum, E. A. Keenan, A. J. Matzger, S. Maldonado, *J. Phys. Chem. C*, 2012, **116**, 3112-3121.
- 17 H. Khajavi, J. Gascon, J. M. Schins, L. D. A. Siebbeles, F. Kapteijn, *J. Phys. Chem. C*, 2011, **115**, 12487-12493.
- 18 S. S. Kaye, A. Dailly, O. M. Yaghi, J. R. Long, *J. Am. Chem. Soc.*, 2007, **129**, 14176-14177.
- 19 M. Sabo, A. Henschel, H. Fröde, E. Klemmb, S. Kaskel, *J. Mater. Chem.*, 2007, **17**, 3827-3832.
- 20 Y. Ming, J. Purewal, J. Yang, C. Xu, R. Soltis, J. Warner, M. Veenstra, M. Gaab, U. Müller, D. J. Siegel, *Langmuir*, 2015, **31**, 4988-4995.
- 21 P. Guo, D. Dutta, A. G. Wong-Foy, D. W. Gidley, A. J. Matzger, *J. Am. Chem. Soc.*, 2015, **137**, 2651-2657.
- 22 D. J. Tranchemontagne, J. R. Hunt, O. M. Yaghi, *Tetrahedron*, 2008, **64**, 8553-8557.
- 23 W. Kraus, G. Nolze, *J. Appl. Crystallogr.*, 1996, **29**, 301-303.
- 24 M. A. Brusa, M. A. Grela, *Phys. Chem. Chem. Phys.*, 2003, **5**, 3294-3298.
- 25 K. M. Choi, H. J. Jeon, J. K. Kang, O. M. Yaghi, *J. Am. Chem. Soc.*, 2011, **133**, 11920-11923.
- 26 C. M. Wu, M. Rathi, S. P. Ahrenkiel, R. T. Koodali, Z. Wang, *Chem. Commun.*, 2013, **49**, 1223-1225.
- 27 J. A. Greathouse, M. D. Allendorf, *J. Am. Chem. Soc.*, 2006, **128**, 10678-10679.
- 28 G. K. Kole, J. J. Vittal, *Chem. Soc. Rev.*, 2013, **42**, 1755-1775.
- 29 J. Canivet, A. Fateeva, Y. Guo, B. Coasne, D. Farrusseng, *Chem. Soc. Rev.*, 2014, **43**, 5594-5617.
- 30 J. J. Low, A. I. Benin, P. Jakubczak, J. F. Abrahamian, S. A. Faheed, R. R. Willli, *J. Am. Chem. Soc.*, 2009, **131**, 15834-15842.
- 31 A. Thirumurugan, C. N. R. Rao, *J. Mater. Chem.*, 2005, **15**, 3852-3858.
- 32 S. Hausdorf, J. Wagler, R. Mossig, F. O. R. L. Mertens, *J. Phys. Chem. A*, 2008, **112**, 7567-7576.
- 33 C. McKinstry, E. J. Cussen, A. J. Fletcher, S. V. Patwardhan, J. Sefcik, *Cryst. Growth Des.*, 2013, **13**, 5481-5486.
- 34 M. Nowak, B. Kauch, P. Szperlich, *Rev. Sci. Instrum.*, 2009, **80**, 046107.
- 35 P. Wurfel, in *Physics of Solar Cells*, Wiley-VCH, Weinheim, 1st edn., 2005, ch. 4, pp. 59-62.
- 36 H. Q. Pham, T. Mai, N. N. Pham-Tran, Y. Kawazoe, H. Mizuseki, D. Nguyen-Manh, *J. Phys. Chem. C*, 2014, **118**, 4567-4577.
- 37 L. M. Yang, G. Y. Fang, J. Ma, E. Ganz, S. S. Han, *Cryst. Growth Des.*, 2014, **14**, 2532-2541.
- 38 M. Ji, X. Lan, Z. Han, C. Hao, J. Qiu, *Inorg. Chem.*, 2012, **51**, 12389-12394.
- 39 P. F. Schwarz, N. J. Turro, S. H. Bossmann, A. M. Braun, A. M. A. A. Wahab, H. Dürr, *J. Phys. Chem. B.*, 1997, **101**, 7127-7134.

SCHEME 1



Scheme 1. Flow chart showing the transition of MOF-5 to MOF-5W and MOF-5H. Middle box shows the proposed structure of MOF-5W. Longer periods of water/moisture exposure give place to the mixture that will be called MOF-5H. Right box shows the structure of TZDH according to ref. 30, which is one of the phases present in MOF-5 H, altogether with MOF-5W.

SCHEME 2



Scheme 2. (a) Scheme of the proposed mechanism for TEMPO photooxidation, (b) Structure of TEMPO and its oxidation product TEMPO⁺, (c) EPR spectrum of TEMPO. The central peak, employed for TEMPO determination is highlighted.

FIGURE 1

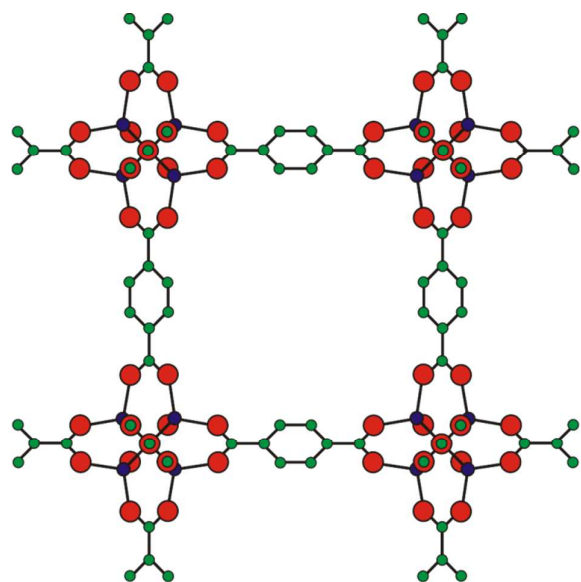


Figure 1. Diagram of the MOF-5 cubic structure. Atoms are coloured in the following way: Zn (blue), Oxygen (red), Carbon (green). Hydrogen atoms are not shown for the sake of simplicity.

FIGURE 2

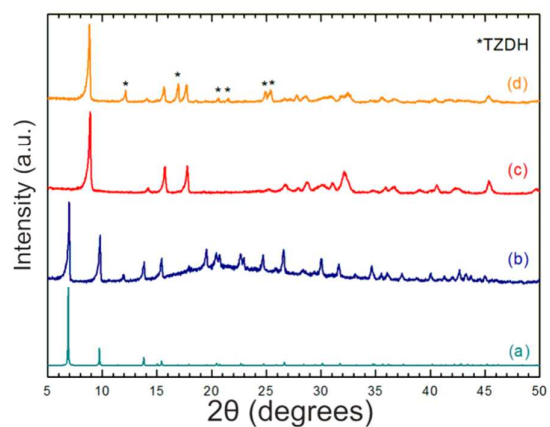


Figure 2. Calculated XRD pattern of MOF-5 (a) and experimental XRD patterns of MOF-5 (b), MOF-5W (c) and MOF-5H (d). The diffraction peaks of TZDH are marked with an asterisk in (d).

FIGURE 3

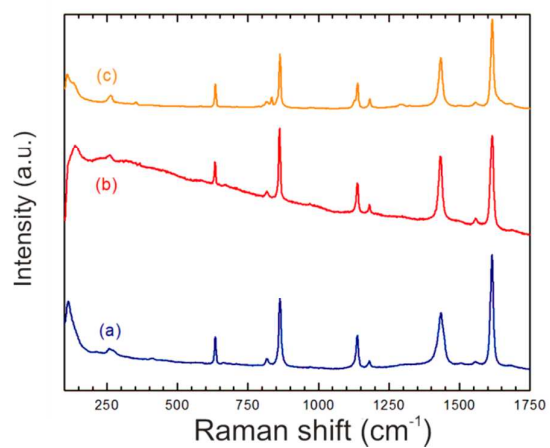


Figure 3. Raman spectra of (a) MOF-5, (b) MOF-5W and (c) MOF-5H.

FIGURE 4

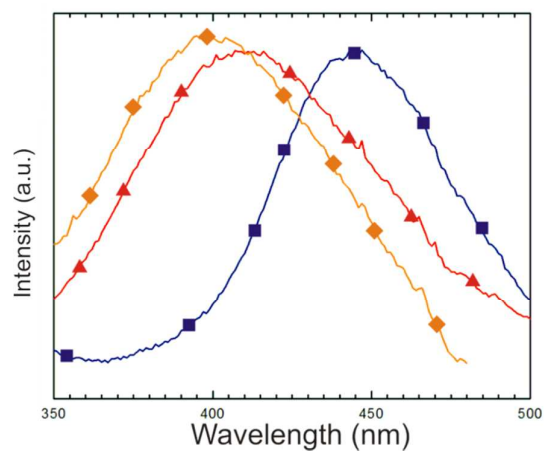


Figure 4. Emission spectra for MOF-5 (blue ■, $\lambda_{\text{ex}} = 325$ nm), MOF-5W (red ▲, $\lambda_{\text{ex}} = 290$ nm) and MOF-5H (orange ◆, $\lambda_{\text{ex}} = 315$ nm).

FIGURE 5

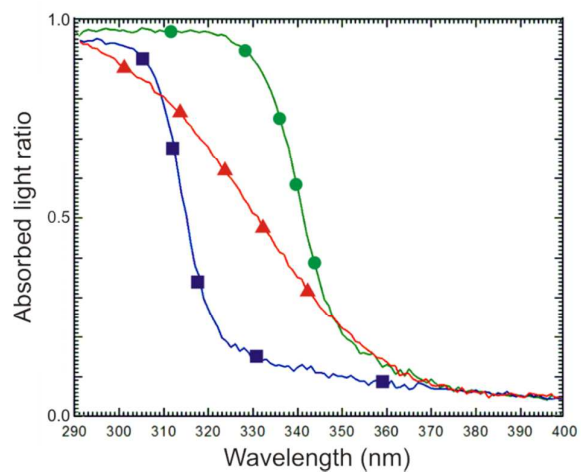


Figure 5. Absorbed light ratio ($A = 1-R-T$) vs. wavelength for MOF-5 (blue ■), MOF-5W (red ▲) and H₂BDC (green ●).

FIGURE 6

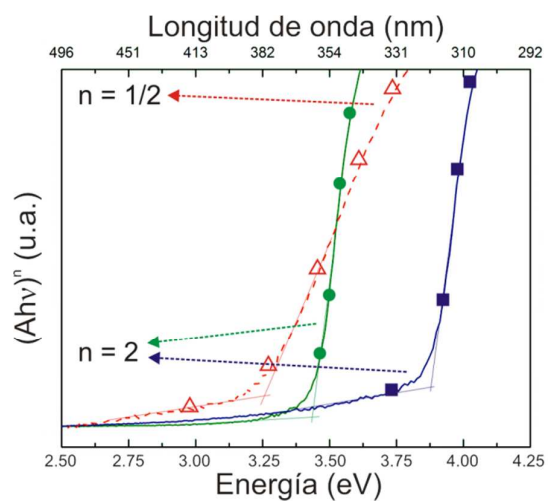


Figure 6. Tauc plots for MOF-5 (blue ■) and H₂BDC (green ●), considered as a direct semiconductors and MOF-5W (red △) considered as an indirect semiconductor.

FIGURE 7

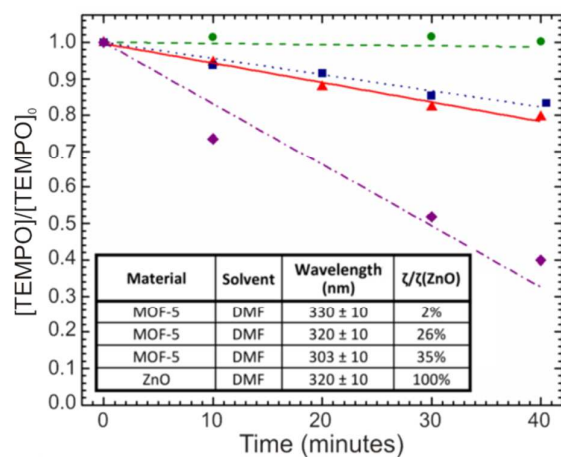


Figure 7. Relative decay of TEMPO observed during the irradiation of an aerated suspension of MOF-5 at 303 nm (blue ▲), 320 nm (red ■) and 330 (green ●) nm. Photooxidation in presence of ZnO at 320 nm (purple ◆) is also shown for comparison.

FIGURE 8

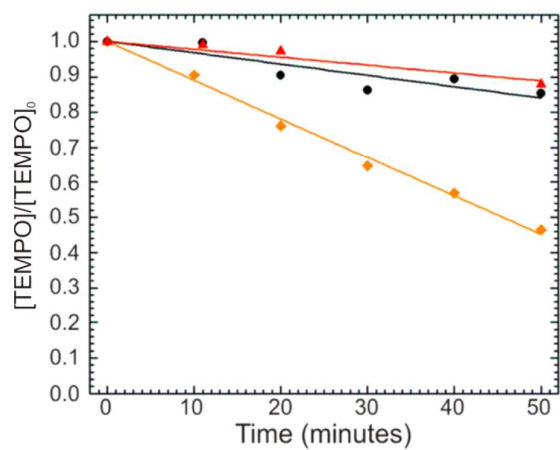
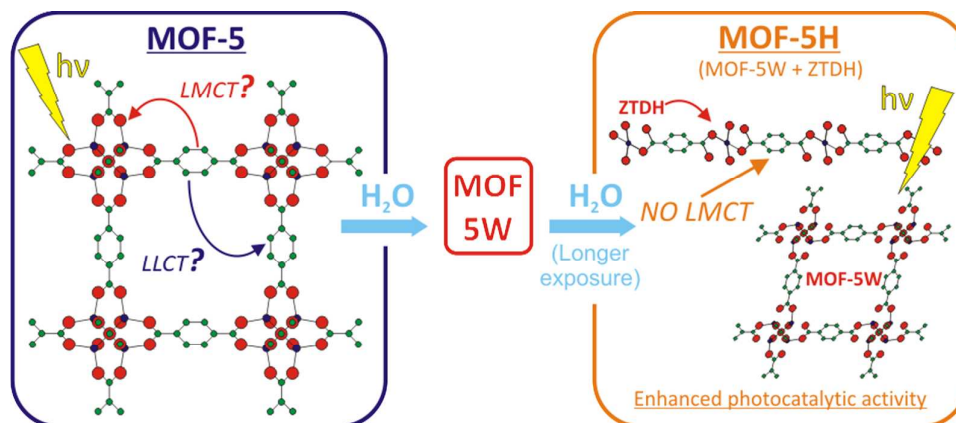


Figure 8. Relative decay of TEMPO observed during the irradiation of an aerated suspension of MOF-5W (red ▲), ZTDH (black ●) and MOF-5H (orange ◆) at 320 nm.

TABLE OF CONTENTS ENTRY.



Hydrolysis of MOF-5 gives place to a mixture of two compounds: MOF-5W and zinc terephthalate dihydrate. The analysis of optical and photochemical properties allows to infer the preeminence of a ligand to metal charge-transfer.